Nuclear Inst. and Methods in Physics Research, A 897 (2018) 54–58

Contents lists available at ScienceDirect

Nuclear Inst. and Methods in Physics Research, A

journal homepage: www.elsevier.com/locate/nima

Optimization of the design of Gas Cherenkov Detectors for ICF diagnosis

Bin Liu [a,b], Huasi Hu [a,*], Hetong Han [c], Huanwen Lv [b], Lan Li [b]

[a] School of Nuclear Science and Technology, Xi'an Jiaotong University (XJTU), Xi'an, 710049, Shannxi, China
[b] Science and Technology on Reactor System Design Technology Laboratory, Nuclear Power Institute of China, Chengdu, 610213, China
[c] North-west Institute of Nuclear Technology, Xi'an, 710049, China

ARTICLE INFO

Keywords:
Inertial confinement fusion
Gas Cherenkov Detector
Genetic algorithm
Monte Carlo simulation

ABSTRACT

A design method, which combines a genetic algorithm (GA) with Monte-Carlo simulation, is established and applied to two different types of Cherenkov detectors, namely, Gas Cherenkov Detector (GCD) and Gamma Reaction History (GRH). For accelerating the optimization program, open Message Passing Interface (MPI) is used in the Geant4 simulation. Compared with the traditional optical ray-tracing method, the performances of these detectors have been improved with the optimization method. The efficiency for GCD system, with a threshold of 6.3 MeV, is enhanced by ∼20% and time response improved by ∼7.2%. For the GRH system, with threshold of 10 MeV, the efficiency is enhanced by ∼76% in comparison with previously published results.

1. Introduction

Inertial Confinement fusion (ICF) is an approach that relies on the inertia of the fuel mass to provide confinement. To achieve conditions under which inertial confinement is sufficient for efficient thermonuclear burn, a capsule containing thermonuclear fuel is compressed in an implosion process to conditions of high density and temperature [1]. Fusion reaction history is strongly dependent on the detailed target hydrodynamics and plasma conditions and is a sensitive indicator of modeling accuracy [2–3]. Two gas Cherenkov detectors, the Gas Cherenkov Detector (GCD) and the Gamma Reaction History (GRH) have been developed by R. R. Berggren and H. W. Herrmann for fusion reaction rate measurements with relatively high efficiency, fast time response and adjustable Cherenkov threshold. GCD operates 20 cm away from the target while GRH operates 6 m away from the target. GRH is placed far away from the fusion gamma source to avoid using the limited measurement aperture while GCD has a larger solid angle due to its proximity to the fusion gamma source. Moreover, GRH can avoid the overlap between Cherenkov signal and signal of γ-rays, secondary electrons and positrons incident directly onto the photocathode of it' s Micro Channel Plate (MCP) [4–5].

As so far, both GCD and GRH systems have been designed by the optical ray-tracing method [6–8]. Based on geometrical optics, the optical ray-tracing method can only be used to trace Cherenkov light. Without considering detailed energy and angular distributions of secondary electrons behind the converter, the performances of the detectors are hard to improve. In the current study, a design method combining GA and Monte-Carlo based code Geant4 is established and applied to the design of the GCD and the GRH. The method couples the γ-rays conversion process with the Cherenkov generation and transmission process, and achieves a global optimization during design process of GCD and GRH. Open Message Passing Interface (MPI) is used to reduce the computational time.

2. The optimization method

The performance of the detection system can be considered as a function of the geometrical or physical parameters of the components in the detection system, which can be expressed as in Eq. (1),

$$y_i = F(x_j),\ i = 1, \ldots, N;\ j = 1, \ldots, M \tag{1}$$

$$x_{j,\min} \leq x_j \leq x_{j,\max} \tag{2}$$

where y_i are the performance of the detection system, such as responses, efficiencies, and so on; x_j are the parameters of the detection components with ranges shown in Eq. (2). As a result, the detector design problem is transformed into a combinational optimization problem. The component parameters of GCD and GRH have been transformed into variables to be constrained by the detection requirements; time response and efficiency are calculated with Geant4 simulation. The optimization is a multi-variable, multi-extremum problem. The gradient based algorithms, such as steepest descent, conjugate gradient, are not able to find the absolute extremum. Genetic algorithm, however, has the advantage of global optimization, so a genetic algorithm is applied [9].

* Corresponding author.
E-mail address: huasi_hu@mail.xjtu.edu.cn (H. Hu).

https://doi.org/10.1016/j.nima.2018.04.032
Received 10 July 2017; Received in revised form 7 April 2018; Accepted 16 April 2018
Available online 30 April 2018

The working process of GCD and GRH can be divided into two stages. During the first stage, the 16.7 MeV gamma-rays incident and generate Cherenkov photons, and the related components are the converter and the gas cell. During the second stage, Cherenkov photons are gathered through the optical reflectors. The optimization has been done in two steps so that GA can do the optimization easier with less optimization parameters than in one step. Firstly, optimization of the geometrical parameters for the converters and gas cells is carried out. Secondly, optimization of geometrical parameters for optical reflectors is carried out based on the optimization results of the converters and gas cells obtained in the first step.

2.1. Optimization of geometrical parameters of converters and gas cells

Assuming the DT fusion source is isotropic, the number of 16.7 MeV γ-rays incident on the converter is given by Eq. (3),

$$N_\gamma = Y_{\gamma DT} \cdot \frac{\Delta\Omega}{4\pi} \tag{3}$$

where N_γ is the number of incident γ-rays on the converter; $Y_{\gamma DT}$ is the yield of 16.7 MeV γ-rays; $\Delta\Omega$ is the solid angle. The optimization objectives are the efficiency and time dispersion of Cherenkov photons collected at the end of the gas cells. Considering the solid angle, the first sub-optimization objective is written as,

$$E_c = N_{cher} \cdot (1 - \frac{d}{\sqrt{r^2 + d^2}}) \tag{4}$$

where N_{cher} is the number of Cherenkov photons collected at the end of the gas cell; d is the distance between the converter and fusion source; r is the radius of the converter.

The time dispersion is given by the variance of the arrival times of Cherenkov photons, as is shown in Eq. (5),

$$\sigma_t^2 = \frac{1}{N_{cher}} \sum_{i=1}^{N_{cher}} (t_i - \bar{t})^2 \tag{5}$$

where t_i is time required by a Cherenkov photon to reach the collecting disk and $\bar{t}$ is average time taken by all Cherenkov photons to reach the collecting disk.

The main purpose of the design process is to optimize geometrical parameters, namely diameters and thicknesses of converter and gas cell. In this way, the time dispersion is minimized and maximum possible Cherenkov photons are obtained. This is a combinational optimization problem with multiple-objectives, and it can be transformed into a single optimization objective using linear weighting method, as given by Eq. (6),

$$Obj = \alpha \frac{E_c(\overrightarrow{X})}{E_{c,\max}(\overrightarrow{X}) - E_{c,\min}(\overrightarrow{X})} + \beta \frac{\sigma^2_{t,\max}(\overrightarrow{X}) - \sigma^2_{t,\min}(\overrightarrow{X})}{\sigma_t^2(\overrightarrow{X})} \tag{6}$$

where α and β are the weight coefficients for detection efficiency and time dispersion. The weight coefficients are determined mainly through experience and by trial and error. Parameters α and β in are set to be 1 and 15 respectively. The terms "$E_{c,\max}(\overrightarrow{X}) - E_{c,\min}(\overrightarrow{X})$" and "$\sigma^2_{t,\max}(\overrightarrow{X}) - \sigma^2_{t.\min}(\overrightarrow{X})$" in Eq. (6), are used to normalize the sub-objectives.

2.2. Optimization of geometrical parameters of optical reflectors

As for the Cassegrain reflectors of GCD, the optimization objectives are Signal to Noise Ratio (SNR) and time dispersion of Cherenkov photons at the collecting disk with diameter of 10 mm. SNR can be represented as given in Eq. (7),

$$SNR = \frac{N_{cher}}{N_{gamma} + N_{elec} + N_{posi}} \tag{7}$$

where N_{cher}, N_{gamma}, N_{elec} and N_{posi} represent the number of Cherenkov photons, γ-rays, electrons and positrons at the collecting surface respectively. The optimization objectives are processed in the same way as described in Eq. (6). The coefficients of SNR and time dispersion are set to be 1 and 40 respectively.

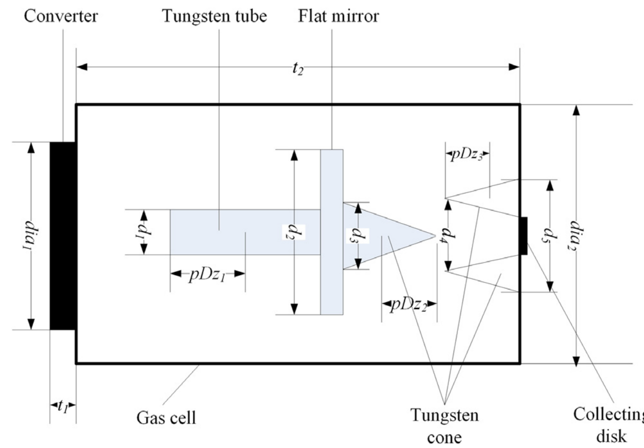

Fig. 1. Schematics of the optimization parameters of GCD.

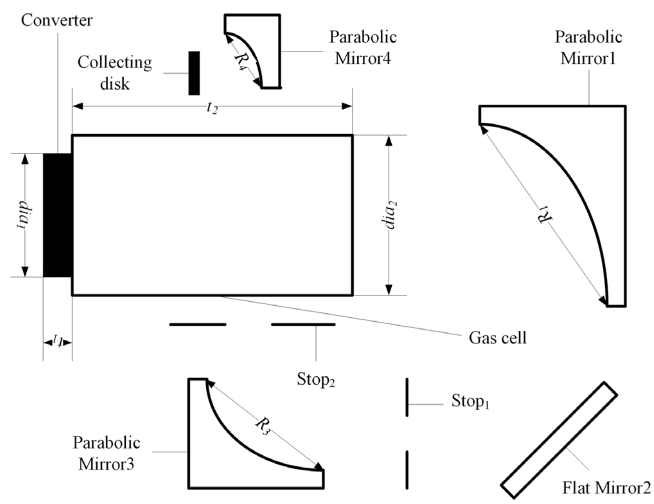

Fig. 2. Schematics of the optimization parameters of GRH.

For off-axis-parabolic reflectors of GRH, the optimization objectives are collection efficiency and the time dispersion of Cherenkov photons at the collecting disk with diameter of 10 mm. The collection efficiency is presented in Eq. (8),

$$E_{collect} = N_{c\_collection}/N_{c\_End} \tag{8}$$

where $N_{c-\,collection}$ is the number of Cherenkov photons at the collecting disk, and N_{c_End} is the number of Cherenkov photons at the end of the optimized gas cell. The optimization objectives $E_{collect}$ and time dispersion are also processed with the linear weighting method by setting coefficients α and β to be 1 and 15 respectively. The optimization parameters of GCD and GRH are shown in Fig. 1.

As is shown in Fig. 1(a), d_1 represents the diameter of the tungsten tube in front of the flat mirror; pDz_1 represents the half thickness of the tube; d_2 represents the diameter of the flat mirror; d_3 represents the diameter of behind the flat mirror and pDz_2 represents half the thickness of the tungsten cone; d_4 and d_5 represent the diameters of the shield part in front of the sphere mirror and pDz_3 represents half the thickness of it; z_1 and z_2 represent the positions of the tungsten tube and the shield part; R represents the radius of the sphere mirror. Constraints of the

Table 1
The optimization parameters of converters and gas cells of GCD and GRH.

Parameter/mm	t_1	dia_1	t_2	dia_2
Range for GCD	0–50	0–80	0–1000	0-80
Results for GCD	18	80	218	80
Range for GRH	0–50	0–150	0–1000	0-150
Results for GRH	26	150	700	150

parameters are presented with inequalities, as shown by Eq. (9),

$$\begin{aligned} & d_1 \leq d_2, d_3 \leq d_2, d_4 \leq d_5 \\ & pDz_1 + pDz_2 + pDz_3 \leq 50 \\ & z_1 + pDz_1 + 2 \cdot pDz_2 - z_2 + pDz_3 \leq -10 \end{aligned} \tag{9}$$

Geometric parameters of the GRH are shown in Fig. 2. Descriptions of these parameters are given in Ref. [10]. The parabolic reflector can be described as the subtraction of a G4Paraboloid from a G4Tubs. Equations for a G4Paraboloid are given in Eq. (10),

$$\begin{aligned} & x^2 + y^2 \leq k_1 \times z + k_2 \\ & -Dz \leq z \leq Dz \\ & R_h^2 = k_1 \times Dz + k_2, \ \ h = 1,3,4 \\ & R_{s2}^2 = k_1 \times (-Dz) + k_2 \end{aligned} \tag{10}$$

Since R_{s2} is set to zero and Dz is fixed, the equation for parabolic mirrors is determined by R_h. Coordinates and rotation matrix of the reflectors are defined by $P_i(x_i, y_i, z_i)$ and $Rot_i(rot_i x, rot_i y, rot_i z)$, where i = 1, 2, 3, 4. Additionally, (x_1, y_1, z_1), (x_2, y_2, z_2) and (y_3, z_3) are fixed to ensure the delay of ~3 ns between the precursor signal and the Cherenkov light signal; $rot_i z$ is zero because of rotational symmetry around the z-axis. Finally, variable θ is introduced for centering the stops, reflector 2, reflector 3, and reflector 4. Then, x_3 and x_4 can be expressed in Eq. (11),

$$\begin{aligned} & x_3 = 140\sqrt{1 + \tan 2\theta} - 200 \tan\theta \\ & x_4 = 140\sqrt{1 + \tan 2\theta} + 150 \tan\theta \end{aligned} \tag{11}$$

In the Geant4 simulation, the optimizations are carried out for 16.7 MeV γ-rays with a Cherenkov threshold of 10 MeV, and 1.65 atm of gas pressure for SF_6. The simulation is done with Geant 4.9.5 [11,12]. The converter and gas cells are made of Be and Al. During the simulation, the absorption length of the Al gas cell is set to zero in order to have all the Cherenkov photons absorbed. In the Geant4 simulation, standard electromagnetic process and optical process are used. The cut value applied for γ-rays, electrons and positrons is 10 μm. The corresponding γ-rays energy thresholds for all of Be, Al and SF_6 is 990 eV. The corresponding electron energy thresholds for Be, Al, and SF_6 are 27 keV, 34 keV, and 990 eV respectively. The dispersion of SF_6, reflectivity of Cassegrain, off-axis parabolic reflectors and transmission of the pressure window were studied by M. S. Rubery [13]. These parameters are adopted in the present Geant4 simulation.

3. Results and discussion

The optimal design of the detectors is obtained using detailed methodology described in Section 2. The results are presented and discussed in detail in following sections.

3.1. Optimization results of converters and gas cells

Considering the different operational conditions of GCD and GRH, the optimization ranges of the converter diameters of GCD and GRH are set to 0–80 mm and 0–150 mm respectively. The ranges and results of the optimization parameters are listed in Table 1.

In Table 1, parameters t_1, dia_1 represent the thickness and diameter of the converter, and t_2 and dia_2 represent the length and diameter of the gas cell. Parameters dia_1 and dia_2 are constrained with the inequality $dia_1 \leq dia_2$.

Table 2
Ranges and results of optimization parameters of reflectors of GCD.

Par/mm	d_1	d_2	d_3	d_4	d_5	pDz_1
Range	0–80	0–80	0–80	0–80	0–80	0-50
Results	10	46	18	36	44	20
Par/mm	pDz_2	pDz_3	z_1	z_2	R	
Range	0–50	0–50	0–1000	0–1000	40–200	
Results	20	8	286	330	121	

As is shown in Table 1, dia_1 and dia_2 reach the maximum values of the range after the optimization. Time responses of the optimization results are shown in Fig. 3.

The uncertainties of the results are given by the statistical uncertainties of the Monte Carlo simulations, which can be evaluated according to Eq. (12). Enough particles are imported into Geant4 code to ensure that R is less than 5%.

$$R = \frac{S_{\bar{x}}}{\bar{x}} = \frac{1}{\sqrt{N-1}}\left[\frac{\overline{x^2}}{\bar{x}^2} - 1\right]^{1/2} \tag{12}$$

The efficiencies of the optimized results are defined by number of Cherenkov photons collected per number of gammas incident on the converter. The efficiency of the optimized results for GCD is 0.11055 ± 0.00038 Cherenkov photons per incident γ-rays with time response of 7.08 ± 0.11 ps, while the efficiency of the 1-meter-long gas cell is $(4.77 \pm 0.02) \times 10^{-2}$ Cherenkov photons per incident γ-rays with time response of 6.25 ± 0.11 ps. After optimization, the efficiency is more than twice as high as the efficiency of the 1-meter-long gas cell, while the time response is 13% worse [14]. Generally, more Cherenkov photons can be produced with a longer gas cell. However, only the Cherenkov photons with appropriate angles can reach the collecting disk; the other Cherenkov photons will be absorbed by the gas cell or the tungsten blocks, so the optimization result of the gas cell for GCD is 218 mm rather than 1 m.

For GRH, the efficiency is $(7.32 \pm 0.02) \times 10^{-1}$ Cherenkov photons per incident γ-rays with time response of 8.70 ± 0.08 ps after optimization. The efficiency of the 50 cm long gas cell is $(6.57 \pm 0.02) \times 10^{-1}$ Cherenkov photons per incident γ-rays with time response of 7.80 ± 0.10 ps [6]. Time response after optimization is deteriorated by 11.54% and efficiency is enhanced by 11.42%.

3.2. Optimization results of optical reflectors

The optimized ranges and results of Cassegrain reflectors of GCD and off-axis-parabolic reflectors of GRH are listed in Tables 2 and 3 respectively.

The optimized results of GCD and GRH are imported into Geant4 code and time responses and efficiency are evaluated. Time responses of the optimization results are shown in Fig. 4. For GCD, the efficiency, calculated by Cherenkov photons collected at the collecting disk at the end of the light collecting system, is $(3.924 \pm 0.009) \times 10^{-2}$ with a time response of 11.20 ± 0.12 ps. The efficiency for 16.7 MeV γ-rays with the threshold of 6.3 MeV (corresponding to SF_6 with gas pressure of 3.95 atm is $(1.601 \pm 0.005) \times 10^{-1}$ Cherenkov photons per incident γ-rays, and the time response is 10.20 ± 0.12 ps. The efficiency is ~20% higher and time response is 0.8 ps smaller than the results obtained by traditional optical ray-tracing method [14,15]. For GRH, the efficiency is $(7.65 \pm 0.03) \times 10^{-2}$ Cherenkov photons per incident γ-rays with the time response of 10.60 ± 0.17 ps. The collection efficiency of the optical reflectors is about 10.44%, which is 5.2% higher than the collection efficiency obtained by the traditional ray-tracing method and time response is deteriorated by 33% [6].

Higher efficiencies for both GCD and GRH are obtained through optimization, shown in Fig. 5. For GRH system, efficiency can be enhanced by about 76% [16]. Considering that the main effect of the detection system related to time response is the photon-electric

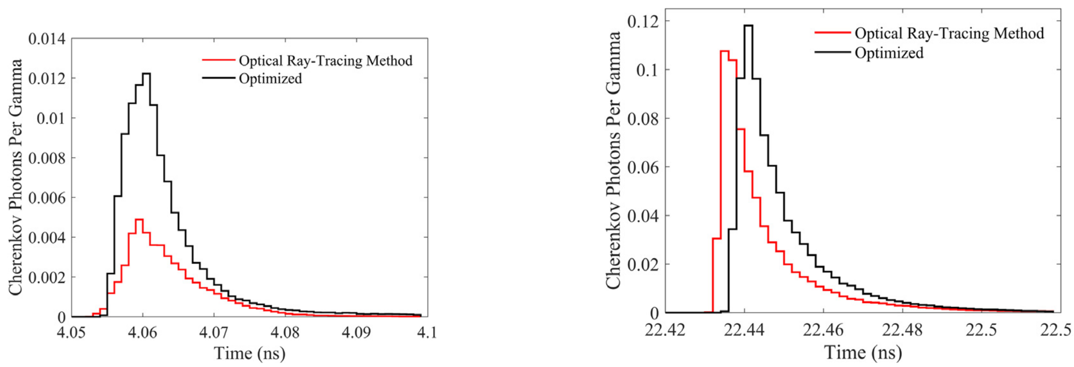

(a) GCD. (b) GRH.

Fig. 3. Time distribution of Cherenkov photons collected at the end of gas cell for GCD (a) and GRH (b). The curves are divided into 50 bins. The optimized curve of Fig. 3(a) is shifted right along time axis by 2.6 ns for comparison, and the 50 cm curve of Fig. 3(b) is shifted left by 0.7 ns for comparison.

Table 3
Ranges and results of optimization parameters for reflectors of GRH.

Par	R_1/mm	rot_1x/deg	rot_1y/deg	rot_2x/deg	R_3/mm	rot_3x/deg	rot_3y/deg
Range	0–150	0–90	160–270	−90–0	0–150	0–90	−90-90
Results	146	43	179	−50	120	46	3
Par	$theta$/deg	rot_4x/deg	rot_4y/deg	y_4/mm	z_4/mm	R_4/mm	
Range	0–20	40–60	160–270	100–200	220–250	30–60	
Results	18	55	194	118	232	33	

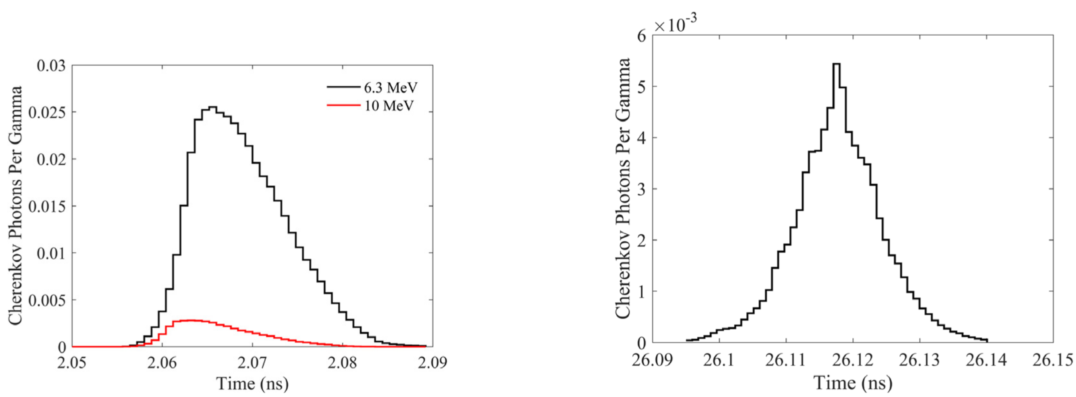

(a) GCD. (b) GRH.

Fig. 4. Time responses of the optimization results of GCD (a) with Cherenkov thresholds of 6.3 MeV and 10 MeV and GRH (b) with Cherenkov threshold of 10 MeV. The curves are divided into 50 bins.

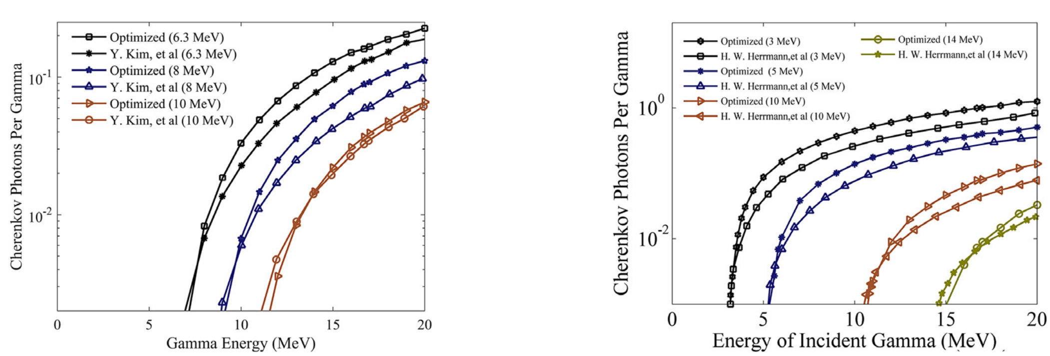

(a) GCD. (b) GRH.

Fig. 5. Energy responses of optimization results of GCD (a) and GRH (b) with comparison of results obtained with optical ray-tracing method.

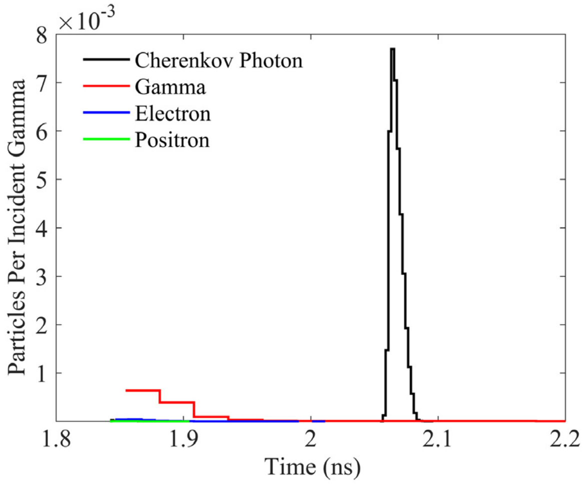

Fig. 6. Time spectrums of Cherenkov photons, γ-rays, electrons and positrons at the collecting disk of optimization results of GCD.

conversion and signal recording systems, the ∼10 ps time response is sufficient for fusion gamma measurement.

Moreover, the time spectra of γ-rays, electrons and positrons which reach the collecting disk of GCD are calculated and the results are shown in Fig. 6. Gamma rays mostly reach the collecting disk before the Cherenkov photons. The SNR of the optimization results of GCD for the whole time range is 24 and SNR under the Cherenkov light signal is 2849, which is sufficient for the detection of 16.7 MeV γ-rays. Moreover, shielding techniques are applied to suppressing noises present during the execution of the experiment, especially at the position of the photo conversion device, such as the Micro Channel Plate Photoelectric Multiplier Tube (MCP-PMT).

3.3. Conclusion

With application of an optimization method, improved geometrical parameters of converters, gas cells and optical reflectors of GCD and GRH are obtained. For the GCD, the efficiency is ∼20% higher and time response is 0.8 ps smaller than the results obtained by traditional optical ray-tracing method. And for the GRH, time response is deteriorated by 33% and the efficiency is enhanced by 76%.

Acknowledgments

The project is supported by the National Natural Science Foundation of China under (10975113 and 11275151) and the Innovative Research Team in University of Ministry of Education of China (Nuclear Energy Science and Engineering, IRT1280).

Appendix A. Supplementary data

Supplementary material related to this article can be found online at https://doi.org/10.1016/j.nima.2018.04.032.

References

[1] J. Lindl, Development of the indirect-drive approach to inertial confinement fusion and the target physics basis for ignition and gain, Phys. plasmas 2 (11) (1995) 3933–4024.

[2] R.J. Leeper, G.A. Chandler, G.W. Cooper, et al., Target diagnostic system or the national ignition facility, Rev. Sci. Instrum. 68 (1) (1997) 868–879.

[3] T.J. Murphy, C.W. Barnes, R.R. Berggren, et al., Nuclear diagnostics for the National Ignition Facility, Rev. Sci. Instrum. 72 (1) (2001) 773–779.

[4] R.R. Berggren, S.E. Caldwell, J.R. Faulkner, et al., Gamma-ray-based fusion burn measurements, Rev. Sci. Instrum. 72 (1) (2001) 873–876.

[5] H.W. Herrmann, C.S. Young, J.M. Mack, et al., ICF gamma-ray reaction history diagnostics, J. Phys. Conf. Ser. 244 (3) (2010) 0320471–0320475.

[6] R.M. Malone, H.W. Herrmann, W. Stoeffl, et al., Gamma bang time/reaction history diagnostics for the national ignition facility using 90°off-axis parabolic mirrors, Rev. Sci. Instrum. 79 (10) (2008) 10E5321–10E5322.

[7] R.M. Malone, B.C. Cox, S.C. Evans, et al., Design and construction of a gamma reaction history diagnostic for the national ignition facility, IEEE Int. Conf. Plasma Sci. 244 (3) (2010) 0320521–0320524.

[8] H.W. Herrmann, J.M. Mack, C.S. Young, et al., Cherenkov radiation conversion and collection considerations for a gamma bang time/reaction history diagnostic for the NIF, Rev. Sci. Instrum. 79 (10) (2008) 10E5311–10E5313.

[9] Z. Michalewicz, Genetic Algorithms + Data Structures = Evolution Programs, Springer, Berlin, 1999.

[10] Bin Liu, Huasi Hu, Tiankui Zhang, et al., Study on Geant4 simulation of GRH system and multiple-objective optimization of optical reflector system with genetic algorithm, Fusion Sci. Technol. 66 (3) (2014) 405–413.

[11] S. Agostinelli, J. Allison, K. Amako, et al., GEANT4-a simulation toolkit, Nucl. Instrum. Methods Phys. Res. A 506 (3) (2007) 250–303.

[12] J. Allison, K. Amako, J. Apostolakis, et al., Geant4 developments and applications, IEEE Trans. Nucl. Sci. 53 (1) (2006) 270–278.

[13] M.S. Rubery, C.J. Horsfield, H.W. Herrmann, et al., Monte Carlo validation experiments for the gas Cherenkov detectors at the National Ignition Facility and Omega, Rev. Sci. Instrum. 84 (7) (2013) 0735041–0735043.

[14] J.M. Mack, R.R. Berggren, S.E. Caldwell, et al., Remarks on detecting high-energy deuterium-tritium fusion gamma rays using a gas Cherenkov detector, Radiation Physics & Chemistry 75 (5) (2006) 551–556.

[15] H.W. Herrmann, Y.H. Kim, C.S. Young, et al., Extended performance gas cherenkov detector for gamma-ray detection in high-energy density experiments, Rev. Sci. Instrum. 85 (11) (2014) 11E1241–11E1243.

[16] H.W. Herrmann, N. Hoffman, D.C. Wilson, et al., Diagnosing inertial confinement fusion gamma ray physics, Rev. Sci. Instrum. 81 (10) (2010) 10D3331–10D3335.